LAWRENCE
LIVERMORE
NATIONAL
LABORATORY

LLNL-TR-628772

# Comments on the Collisionless Shock Experiments

D. D. Ryutov

March 20, 2013

## Disclaimer



This work performed under the auspices of the U.S. Department of Energy by Lawrence Livermore National Laboratory under Contract DE-AC52-07NA27344.

*Technical report* *March 19, 2013*
*LLNL-TR-628772*

# Comments on the collisionless shock experiments[1]

D.D. Ryutov, LLNL

**Shocks on a platform of two counterstreaming plasmas**

Let's compare the shock-tube experiment with ordinary collisional shocks (Fig. 1) and an imaginary shock-tube experiment with the collisionless shocks in the counterstreaming plasmas (Fig. 2).

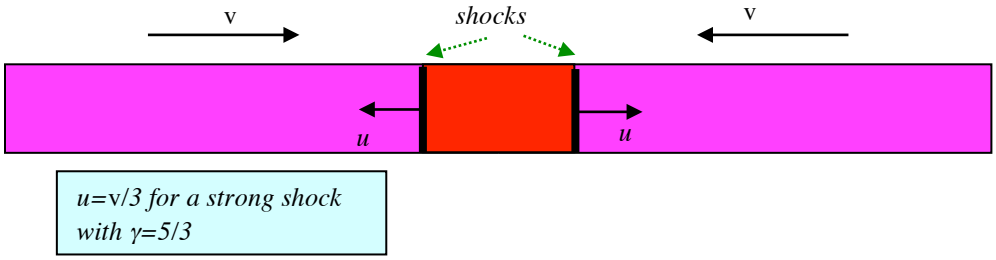


Fig. 1 Shown in red is a resting shocked material. The temperature is of order of a directed energy per particle.

If well-developed collisionless shocks are formed, with the dissipation on the shock front mediated by the microturbulence, then we are looking at the structure shown in Fig. 1. There are two shocks, separated by the region of a shocked material. The shock thickness is

$$l^* = K\frac{c}{\omega_{pi}};\quad l^*(cm) \approx K\frac{3\times 10^7}{\sqrt{n_e(cm^{-3})}}, \qquad (1)$$

where $K$ is a numerical coefficient that is greater than 30 as the present experiments with OMEGA clearly show. [What allows us to make this statement, is the fact that in the

[1] This work was performed under the Auspices of the U.S. Department of Energy by Lawrence Livermore National Security, LLC, Lawrence Livermore National Laboratory, under Contract DE-AC52-07NA27344

Omega experiments the ion temperature has not been anywhere close to the Rankine-Hugoniot temperature, see Ref. 2 and Appendix 1.] Determining how large $K$ actually is, is the goal of our experiments.

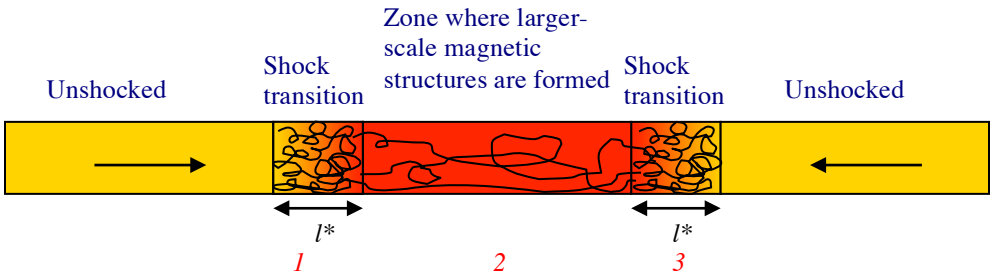


Fig. 2 This is an imaginary shock-tube version of the collisionless shock experiment.

In Fig. 2, we have two shocks separated by a stagnant region. As the ions become quasi-isotropic here, the instability drive turns off, and the microturbulence decays. Most probably, the shortest wavelengths decay first, leaving "alive" only large-scale structures. The latter, situated in zone 2, are suitable for producing the proton images. [Note that there is a viewpoint that the magnetic field may die away almost completely, Ref. 1]. As $K$ is greater than 30, the shock transitions 1 and 2 cover at least 30 fastest-growing scales each. Therefore, the effect of these transition regions on the proton beam is mostly the beam *scattering*, not a regular deflection (the beam passes through at least 30 randomly-distributed structures). So, one can expect that the proton beam sent through zones 1 and 3 will be blurred, with some angular divergence of the scattered beam $\theta \equiv \left\langle \vartheta^2 \right\rangle^{1/2}$. As the fluctuations that scatter the proton beam are the same as those that scatter the ions of the main counterstreaming plasmas, one can relate $\theta$ and the shock thickness $l$*:

$$\theta \sim \sqrt{F \frac{l}{l^*} \left( \frac{\mathrm{v}}{\mathrm{v}_p} \right)^2} , \qquad (2)$$

where $l$ is the path of the proton beam through the plasma, v is the velocity of the plasma stream, $\mathrm{v}_p$ is the proton velocity, and $F$ is a form-factor depending on the details of the turbulent spectrum. This prediction can (and should) be made more quantitative; requires some (modest) effort. Assuming that $F$~1, $l/l$*~1, v=$10^8$ cm/s and 10 MeV protons, one

finds $\theta \sim 1/40$. For our standard distance of 1 cm between the proton source and the object, this means that all the structures with the size less than 250 μm will be blurred.

The scattering can be considered as a nuisance, but may in fact become a yet another tool for the studies of the plasma turbulence (somewhat analogous to the Thomson scattering). The specific detection technique needs discussion. One obvious approach would be to use a mesh made of wires of different thickness, say, from 10 microns to 300 microns. One can expect that the thinnest wires will be blurred, whereas the thick one will be clearly visible. The transition between the two would allow one to make an estimate of the scattering angle.

If large-scale magnetic structures are formed, the best chance to see them is zone 2, where the scattering becomes insignificant or, perhaps, in the transition regions from zones 1 and 3 to zone 2, where the turbulence start decaying and the large-scale structures emerge. By the large-scale structures I mean the structures with the sptial scale comparable to $l^*$ or a few times less than $l^*$. The imaging of these large-scale structures imposes constraints on the duration of the probe beam. Denoting the characteristic variability time of these structures as $\tau$, we have to have a probe beam whose duration is significantly less than $\tau$. For the structures formed by the ion Weibel instability the time $\tau$ should be of order of the structure size over the stream velocity v. For the structures of order of $l^*/3$ or greater, one has $\tau > l^*/3v$. So, we impose the following constraint on the probe beam duration:

$$\tau_{probe} << l^*/3v \quad . \tag{3}$$

For $l^*=1$ mm and $v=10^8$ cm/s, this constraint reads as $\tau_{probe} << 300$ ps. This condition is usually satisfied for the $DHe^3$ source.

**Seeding the perturbations in order to facilitate the shock formation**

The difficulty of the collisionless shock experiment is related to the potentially large value of the coefficient $K$, Eq. 1. One can try to facilitate the instability development by seeding the plasma with initial perturbations, which will be weaker than those developed at the final stage of the turbulence but stronger than those present in the "natural" environment. An additional advantage of imposing controlled perturbations

may be an opportunity to test the predictions of the instability growth. This technique is very common, e.g., in the studies of the interface instabilities (Remington et al, 1995, Ref. 3).

The fastest growing modes have a length-scale ~$c/\omega_{pi}$. For our typical electron density in the midplane ~$10^{19}$ $cm^{-3}$ the scale length in the midplane is ~ 30 μm. If we want to seed perturbations as the surface ripples of a large amplitude on the target, we would have to account for the spherical divergence of the flow. Under typical conditions, the diameter of the flow in the midplane is ~3000 – 4000 mm. The number of the scale-lengths over this scale is therefore ~ 100 (see Kugland, PoP, invited, Ref. 4). The number of the wavelengths across the diameter is $100/2\pi \sim 15$. For the 300 μm spot diameter, this corresponds to 15 wavelengths with $\lambda$=20 μm. As the focal spot is a 2D object, the total number of bumps and dimples will be $15^2$~200. The perturbations should be significant, with the peak-to-valley amplitude ~ $\lambda/2$ or so. For the weaker perturbations the concern is that they will be washed away on their way to the midplane. The large peaks will probably create higher plasma density and flow velocity than the valleys. A local Biermann battery effect may even seed them with the manetic field with the structure characteristic of the filaments. One relatively straightforward way would be to use a target assembled of the "gramophone needles." Another approach would be to use the laser beam with deliberately introduced tightly-spaced speckles, ~ 200 in total within the imprint.

There will inevitably be a degree of empiricism in this exercise, but the possibility that it will give rise to a robust shock and the flow stagnation in the midplane makes it worth trying, possibly with consultation from those who worked with the egg-crate and other types of the seed.

**Effects of the real geometry**

The sketches of Fig. 1 and Fig. 2 correspond to one-dimensional system that can be realized in the shock-tube experiments. In our case we have two counterstreaming plasma flows in the open space. Therefore, if the interaction is strong, shocks are formed and the hot, quasi-isotropic plasma appears in a would-be stagnation zone. The hot plasma starts

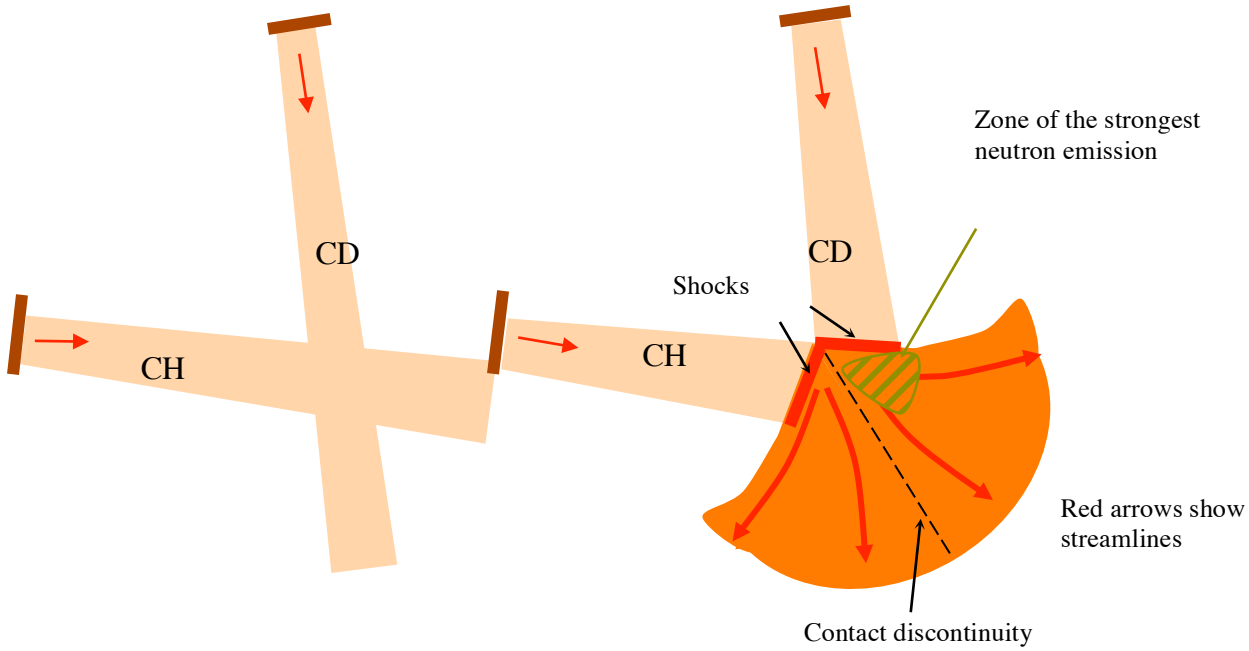


Fig.3 The difference between a free penetration of two plasma streams through each other and their behavior when well-deveoped collisionless shocks are formed. See further explanations in the text.

to expand in the lateral direction, with the velocity comparable to that of the initial streams. It is somewhat similar to what happens if the jets from two firehoses collide. Fig. 3 is a sketch illustrating the point for the case where two streams intersect at some angle.

A similar sketch depicting the head-on collision is presented in Fig. 4. The measure of success in this case could be the density and velocity of the plasma at some distance from the axis at the midplane. In the case of a weak interaction, the result would be very similar to S. Ross' Thomson scattering results, Ref. 2, with two clearly distinguishable interpenetrating ion flows, each of the same density as a single flow. In this regard, the TS is as powerful tool as the proton deflectometry. The difference is that the latter can probably distinguish between electric and magnetic fluctuations. On the

other hand, the theory predicts quite clearly that significant interaction can not occur due to the electrostatic instability alone.

Note that in the geometry of Fig. 4 it is hard to assume that the magnetic field in the shocked region will be aligned with the direction of any of the initial flows. So, the large-scale field structures in the shocked zone will probably be quite complex.

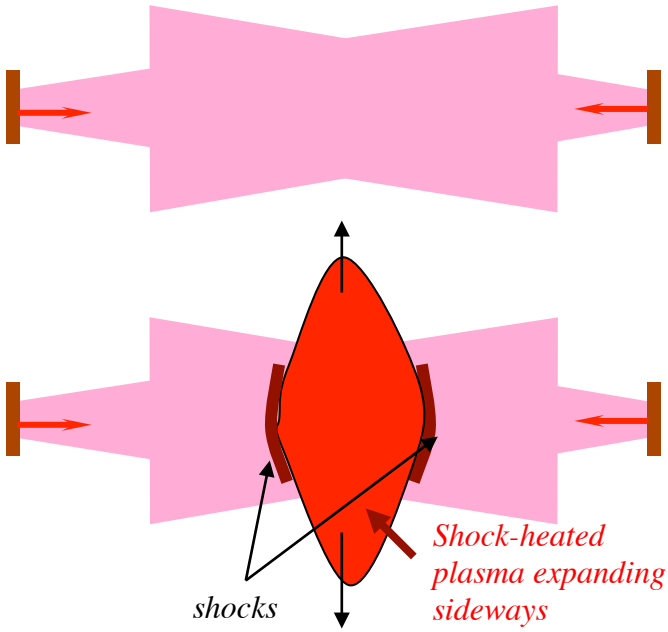


Fig. 4 Upper panel: two diverging plasma streams freely penetrating through each other. Lower panel: strong collisionless shocks are formed; the shock-heated plasma (red) expands laterally

**Neutron Diagnostic**

As there is no TS diagnostic on NIF, we have to rely on other tools. One of them could be a neutron diagnostic, with the use of two streams made of $CH_2$ and $CD_2$, respectively, Fig. 3. In this setting ($CH_2$ colliding with $CD_2$), only strong shock heating would lead to the neutron signal. For the parameters of plasma streams anticipated for NIF, the well-developed shock should produce sufficient number of DD neutrons.

**Reducing the role of large-scale toroidal fields**

Intriguing pancake-like structures observed in the proton deflectometry in Ref. 4 may be related to the Biermann Battery effect acting near the targts, with the field generated there advected by the electron flow and partially recompressed near the midplane [5]. This effect can be substantially reduced by the transition to the larger-radius focal spots. One of the spatial scales increases substantially, and the problem becomes almost one-dimensional (Fig. 5).

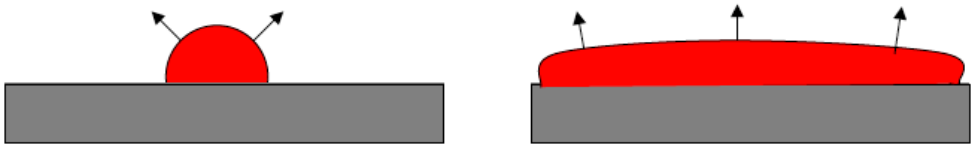

Fig. 5 A sketch illustrating an early stage of the plasma expansion from a small spot (left panel) and large spot (right panel).

The larger-scale structure may be also more amenable to the introduction of perturbations.

**Pulse-shaping and single target approach**

By using a laser pulse consisting of a relatively long pulse followed by a significantly shorter and more intense pulse, one can generate a plasma cloud (by the long pulse) into which a plasma pusher produced by the short pulse would propagate. This may allow us to have a system with one target and thereby providing a much better diagnostic access.

**Knock-on protons and deuterons**

The Coulomb collisions cause the change of the distribution function predominantly via the small-angle, "diffusive" scattering, as reflected by the presence of the Coulomb logarithm in the collision frequencies. However, a small-impact-parameter collisions do also take place and may cause effects potentially usable for the diagnostic purposes. We show here that such "close" collisions of light ions of one of the streams with carbon ions

of the other stream can produce light ions with a significant energy, exceeding the initial energy of the light ions by a factor of 5-6.

We provide an expression for the maximum proton energy produced in such a process. This energy corresponds to a head-on collision of the proton with the velocity v and the heavier ion moving in the opposite direction with the same velocity. We denote the atomic weight of the heavy ion by $A_H$ and the atomic weight of the light ion by $A_L$. From the momentum conservation, one readily obtains the following expression for the recoil energy of the light ion:

$$W_L' = \frac{A_L}{A_H}\left(\frac{3A_H - A_L}{A_H + A_L}\right)^2 W_H \quad , \qquad (4)$$

where $W_H$ is an energy of a heavy ion before the collision, $W_H=A_H m_p v^2/2$. For the protons colliding with carbon ions, $W'_P=0.6W_C$; for the deuterons $W'_D=0.98W_C$. In other words, in the CH or CD plasma streams with the velocity of $10^8$ cm/s, the protons with the energy up to 36 keV and the deuterons with the energy close to 60 keV would be formed. [Their "flow" energies are 5 and 10 keV, respectively.]

Of course, the light particles with lower energies will also be formed for the collisions different from the head-on collisions and thereby leading to formation of particles moving at some angle with respect to the axis of the streams. The energy and angular distributions can be expressed in a closed form. The fraction of the fast particles with the energies between the aforementioned maximum and ½ of the maximum will be $\sim 10^{-3}$ of the total number of particles in each stream (more accurate estimate requires time).

**Appendix 1 Rankine-Hugoniot stagnation temperature for collisional shocks with *M*>>1**

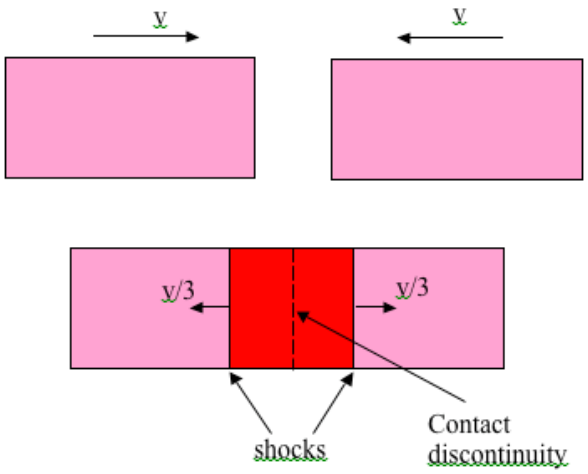


Fig. 6 Symmetric (identical) flows with the incoming velocity v

Post-shock density $n_e^* = 4n_e$ (asterisk marks post-shock quantities).

Consider first a single-component flow (say, carbon). The post-shock ion temperature depends on whether e-i temperature equilibration occurred, or not. For cold electrons (no equilibration) $p^* = \frac{n_e^*}{Z} T_i^*$, so that

$$T_i^* = \frac{Am_p \mathrm{v}^2}{3} = \frac{2}{3} W_i$$

For equal electron and ion temperatures $p^* = \left(1 + \frac{1}{Z}\right) n_e^* T^*$, so that

$$T_i^* \left(= T_e^*\right) = \frac{Am_p \mathrm{v}^2}{3(1+Z)} = \frac{2}{3(1+Z)} W_i; \qquad W_i\left(keV\right) = 5.2 \times 10^{-16} A \left[\mathrm{v}\left(cm/s\right)\right]^2$$

For $CH_2$, in the case of no equilibration between electrons and ions (but equal temperatures of C and H)

$$T_i\left(keV\right) = \frac{28}{9} \times 5.2 \times 10^{-16} \left[\mathrm{v}\left(cm/s\right)\right]^2 = 1.62 \times 10^{-15} \left[\mathrm{v}\left(cm/s\right)\right]^2$$

For $CH_2$, in the case of complete equilibration between electrons and ions

$$T_i\left(keV\right) = \frac{28}{33} \times 5.2 \times 10^{-16} \left[\mathrm{v}\left(cm/s\right)\right]^2 = 4.4 \times 10^{-16} \left[\mathrm{v}\left(cm/s\right)\right]^2$$

## References


1. Jaehong Park, Chuan Ren, et al. Phys. Plas., **17**, 022901 (2010).
2. J.S. Ross et al. Phys. Plas., **19**, 056501 (2012).
3. B.A. Remington et al. Phys. Plas., **2**, 241 (1995).
4. N.L. Kugland et al. Phys. Plas. **20**, #5 (2013).
5. D.D. Ryutov et al. Phys. Plas. **20**, 032703 (2013)